Protein and lipid characterization of wheat roots plasma membrane damaged by Fe and H_2O_2 using ATR-FTIR method

Xin Zhao[1,2*], Xiaoju Yang[1,2], Yong Shi[1,2], Guoxiong Chen[1,2], Xinrong Li[1,2]

[1]Key Laboratory of Stress Physiology and Ecology, Lanzhou, China; [*]Corresponding Author: zhaox@lzb.ac.cn
[2]Shapotou Desert Research Station, Cold and Arid Regions Environmental and Engineering Research Institute, Chinese Academy of Sciences, Lanzhou, China

ABSTRACT

In plant cells the plasma membrane is a highly elaborated structure that functions as the point of exchange with adjoining cells, cell walls and the external environment. In this study, we investigated the structure and function characteristic of wheat root plasma membrane (PM) as affected by H_2O_2 and Fe by using fluorescence spectroscopic and attenuated total reflectance infrared (ATR-IR) techniques. The results showed that these oxidant damaged induced an obviously reduced membrane fluidity were observed in the roots PM treated with the 200 µM H_2O_2, $FeSO_4$, and $FeCl_3$. Computer-aided software analyses of the FTIR spectrum indicated that the content of the α-helices decreased and β-sheet increased in the secondary structures of proteins after exposure to the oxidants of 200 µM H_2O_2, $FeSO_4$, and $FeCl_3$. The number of P=O and C=C bonds area declined rapidly in the lipids of the membrane under the oxidants stress. These structural alterations might explain the reason of the roots PM instability under most of the abiotic stress.

Keywords: Plasma Membrane; Fourier Transforms Infrared (FTIR); Attenuated Total Reflectance (ATR); H_2O_2; Iron

1. INTRODUCTION

Plant cell membrane is the thin layer of protein and fat that surrounds the cell. The cell membrane is semi permeable, allowing some substances to pass into the cell and blocking others. In plant cells, the plasma membrane is a highly elaborated structure that functions as the point of exchange with adjoining cells, cell walls and the external environment. Plants show a great ability to adapt their metabolism to rapid changes in the environment. Most transport proteins in plant cells are energized by electrochemical gradients of protons across the plasma membrane. Plants are prone to produce excessive reactive oxygen species (ROS) under adverse conditions such as drought, extreme temperature, high irradiance, atmospheric pollution, pathogen attack, etc. ROS includes singlet oxygen (O_2^1), superoxide radical (O_2^-), hydrogen peroxide (H_2O_2) and hydroxyl radical (HO^-). They are considered to be toxic byproducts of aerobic metabolism because they can react with various cellular components to induce oxidative damage [1]. Current evidence suggests that OH and H_2O_2 cause damage to cells by the generation of potent oxidizing species. Previous studies [2-4] have indicated that oxygen radicals and other activated oxygen species such as H_2O_2 can increase protein degradation in intact cells and intracellular organelles, as well as *in vitro* systems. OH and H_2O_2 are known to damage various proteins by inducing oxidative modification, non-enzymatic fragmentation, and aggregation, or indirectly by peroxidation of membrane phospholipids [2].

Iron is an essential element in the prosthetic groups of many constituents of photosynthetic electron transport carriers and enzyme factors [5]. However, excess iron severely restricts cellular growth and results in a variety of morphological symptoms, among which the best characterized is leaf bronzing on crop plant [6-8]. Among heavy metals, Fe^{2+} and Cu^{2+} ions, normally occurring in the cells, can react with H_2O_2 and OH^- is formed via the Haber-Weiss reaction. Sills found that a strong oxidant effect can decrease the number of C=C bonds in phospholipids of the plasma membranes [9]. Yang reported that both $FeSO_4$ and $FeCl_3$ significantly inhibited the roots PM H^+-ATPase activity, and the inhibition could be reversed by the addition of the metal ion chelator EDTA-Na_2 or a specific Fe^{2+} chelator, indicating that the inhibitory effect was due to specific action of Fe^{2+} or Fe^{3+}. Measurement of the extent of lipid peroxidation showed that oxidative damage on the roots PM caused by

Fe^{2+} or Fe^{3+} seemed to be correlated with the inhibition of the roots PM H^+-ATPase activity of the roots PM vesicles isolated from wheat roots[10] . But what is the reason of H^+-ATPase activity changed, and whether the roots PM vesicles structure was changed too. And what is the protein and lipid characterization of wheat roots plasma membrane affected by iron damaged.

Attenuated total reflection Fourier transform infrared spectroscopy (ATR-FTIR) is one of the most powerful techniques for recording the infrared spectra of biological materials in general, and for biological membranes in particular. It is rapid, yields a strong signal with only a few micrograms of sample and, most importantly, it allows information about the orientation of various parts of the molecule under study to be evaluated in an oriented system. The environment of the molecules can be modulated so that their conformation can be studied as a function of temperature, pressure, and pH, as well as in the presence of specific ligands. Because of the long IR wavelength, light-scattering problems are virtually nonexistent, and highly aggregated materials or large membrane fragments can be investigated. A unique advantage of infrared spectroscopy is that it allows simultaneous study of the structure of lipids and proteins in intact biological membranes without the disturbance caused by the introduction of foreign probes [11]. It has been claimed that some types of analysis of infrared data can provide highly accurate quantitative estimates of the secondary structure content, with a standard deviation as low as 2% - 3% with respect to the corresponding X-ray structures. The advantage of FTIR is that protein secondary structure is measured in the native environment of the proteins and that it is a noninvasive technique [9,12]. Differences in the C=O stretching vibrations of the peptide groups (the amide I region between 1600 and 1700 cm^{-1}) can provide information on types of secondary structure, such as *α*-helix, *β*-strands, and different kinds of turn structures [13].

In this report, we examined the response to iron and H_2O_2 damage on the roots PM fluidity, investigated the protein secondary structure and phospholipids conformation in the roots PM vesicles from wheat roots. In order to found protein and lipid characterization of wheat roots plasma membrane affected by Fe and H_2O_2. Therefore we could understand the mechanisms of plant growth and survival in hostile environments at the molecular and plant-cell level.

2. MATERIALS AND METHODS

2.1. Plant Materials

Wheat seeds (*Triticum aestivum* L., variety Longchun No. 20, purchased from Gansu Academy of Agricultural Sciences, China) were sterilized with 1% sodium hypochlorite (NaClO) solution for 20 min, then soaked in water for 2 h and germinated in the dark at 25°C for 24 h; the seedlings were grown in quartz sand and irrigated with tap water. The wheat seedlings, illuminated for 14 h every day at a light intensity of 150 μmol·m^{-2}·s^{-1}, were grown for 10 days at 21°C.

2.2. Plasma Membrane Isolation, Purification, and H_2O_2 and Iron Treatments

The PM-enriched vesicles were prepared as described by Kasamo [14] with some modifications. Wheat roots were collected, washed cleaning and cut into pieces and immediately homogenized in the isolation medium containing Hepes/Tris 50 mM (pH 7.5), and Sucrose 250 mM (with EDTA 1 mM, PVP 0.6%, PMSF 1 mM, and DTT 1 mM). The homogenate was filtered through four layers of cotton gauze and centrifuged at 15,000 g for 15 min. The supernatant was then centrifuged for 40 min at 80,000 g in order to obtain a membranes microsomal pellet, which was resuspended in a buffer containing 0.048% potassium phosphate (pH 7.8). All steps were carried out at 4°C in a cold room.

The roots PM vesicles were isolated by a two-phase aqueous polymer preparation system [15] with some modifications. Protein concentration was determined by the method of Coomassie brilliant blue G-250 staining [16] and using with bovine serum albumin as the standard. Every 20 ug of plasma membrane pellets were used immediately to add in 200 μM H_2O_2, $FeSO_4$ and $FeCl_3$ solution (D_2O buffer solution) for 30 min in an ice box.

2.3. Assay of the Roots PM Fluidity

Plasma membrane fluidity of treatment with 200 μM H_2O_2, $FeSO_4$ and $FeCl_3$ solution for 30 min was determined according to the method of Zhang's [17]. An amount of 3 mL of medium would contain 282 mM mannitol (pH 7.2), 50 μM 8-anilino-1-naphthalene -sulfonic acid (ANS, as a fluorescence probe), and 20 μg of protein preparation of plasma membranes. Before the determination of plasma membranes fluidity, it was necessary to determine protein concentrations in the preparation of plasma membranes isolated from wheat roots grown in nutrient solutions. ANS was added and mixed, and 2 min later fluorescence intensity was measured with a fluorescence spectrometer (Phillips 4101) at 22°C. Emission and excitation wavelengths were 390 nm and 473 nm, respectively.

2.3. ATR-FTIR Spectroscopy Measurements and Data Analysis

$FeSO_4$, $FeCl_3$ and H_2O_2 were dissolved in an identical concentration but D_2O-based buffer. To remove the spectral interference from H_2O absorption bands (OH$^-$ bond

strongly absorbed on amide I 1600 - 1700 cm^{-1}). The roots PM sample was treated with 200 μM Fe^{3+}, Fe^{2+} and H$_2$O$_2$ for 30 min at 4˚C. The samples were layered on CaF$_2$ windows then allow to dry under vacuum in the dark. The infrared measurements were performed with a Fourier transform infrared spectrometer with OMNI sampler (Nexus 670; Nicolet, Madison, WI, USA) with germanium plane in a 2 mm^2 sensing area. Attenuated total reflection infrared (ATR-FTIR) spectra were recorded with OMNIC software. The internal reflection element was a germanium ATR plate (50 × 20 × 2 mm) with an aperture angle of 45˚. A total of 128 scans were accumulated for each spectrum. Spectra were recorded at a nominal resolution of 2 cm^{-1}.

Spectral analysis and display were carried out using the IR Data Manager analytical software of OMNIC (Version 6.0, Nicolet, USA), which was used to obtain original and Fourier self-deconvolution spectra and second-derivative spectra.

The parameters for the Fourier self-deconvolution procedure were a smooth factor of 15.0 and a width factor of 30.0 cm^{-1}, using the interactive Fourier self-deconvolution function of OMNIC 6.0. The line width in the deconvolved spectrum was chosen carefully to avoid the introduction of erroneous bands [18]. The second-derivative spectrum was normalized, and the band position was calculated as the average of the spectral positions at 80% of the total peak height. These were smoothed over 15 data points.

The water spectra to be subtracted were collected under the same conditions as the membrane spectra. Criteria for the correctness of subtraction were removal of the band near 2200 cm^{-1} and flat baseline between 1800 and 2000 cm^{-1} for samples in H$_2$O, and elimination of the strong band at 1209 cm^{-1} for samples in D$_2$O avoiding negative side lobes. Second-derivative and deconvolution spectra were used to determine the number and the positions of the bands as starting parameters for the curve-fitting procedure, assuming Pearson or Voigt band shapes.

The curve-fitting bands were selected using Origin 7.0 software with an appended PFM (peak fitting maximum) function; for protein studies the spectral region between 1800 and 1500 cm^{-1} were selected. This region contains the amide I and amide II absorption bands of the protein backbones. Band curve-fitting includes the decomposition of the amide I band into its constituents and the assignment of these components to protein structural features. To start the quantification process, the number and position of the bands and a rough estimation of band shapes, widths and heights of the components is needed. The Gaussian peak shape was used to fit the spectrum collected at each time point (chi-squared X^2 < 10^{-5}). Band curve-fitting is best performed on original bands, although it is sometimes accomplished, less accurately,

on more shapely spectra obtained through self-deconvolution or second derivation.

3. RESULTS

3.1. Iron and H$_2$O$_2$ Induced Decline Fluidity of the Roots PM

The fluorescence intensity of the roots PM damaged by H$_2$O$_2$ and Fe were shown in **Figure 1**. It was showed that the ANS fluorescence intensity of treated with 200 μM H$_2$O$_2$ was almost double times than that untreated the roots PM vesicles, but the fluorescence intensity values of the roots PM treated with 200 μM Fe^{2+} and Fe^{3+} were appeared a little bit higher than that of untreated the roots PM vesicles, indicating a little bit stronger of damage. This suggests that plasma membrane hydrophobization decreased strongly with H$_2$O$_2$ oxidation damage.

3.2. The Protein and Ester Content Change of the Damaged the Roots PM

From **Figure 2(a)**, it is showed that the FTIR original spectral lines of the roots PM treated with oxidant of 200 μM H$_2$O$_2$, Fe^{2+} and Fe^{3+} were similar. From the 1742 cm^{-1} - 1720 cm^{-1} absorption bands indicate stretching vibrations of the content of C=O, or ester region, in membrane lipids. From 1600 - 1700 cm^{-1} band area is assignment to Amide I of the protein contents [19]. Using band area measure tool of OMIC softerware, we found from **Figure 2(b)** that the Amide I content of the roots PM in Fe^{2+}, H$_2$O$_2$, and Fe^{3+} treated only remain of 87%, 33%,
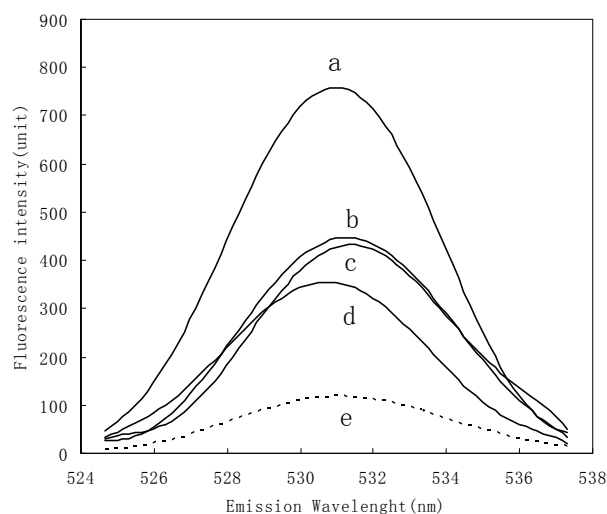
Figure 1. Effects of H$_2$O$_2$, Fe^{2+}, and Fe^{3+} on changes in membrane fluidity. Fluorescence spectra of the roots PM vesicles damaged with 200 μM H$_2$O$_2$, Fe^{2+}, and Fe^{3+} applied at 4˚C for 30 min (ANS as the fluorescence probe). The five curves represent the following treatments: a) ANS + PM + 200 μM H$_2$O$_2$, b) ANS + PM + 200 μM Fe^{2+}, c) ANS + PM + 200 μM Fe^{3+}, d) ANS + PM, e) ANS.
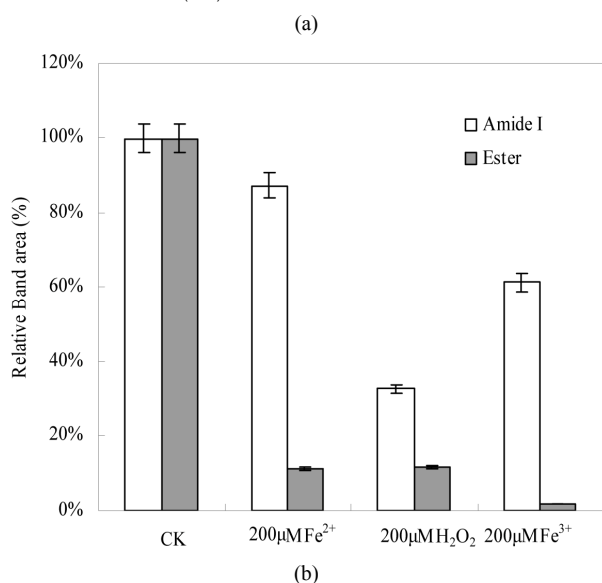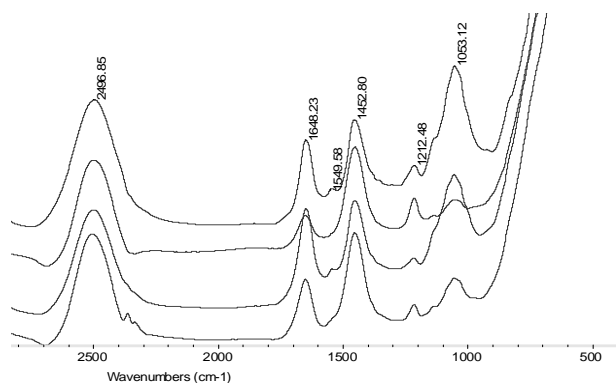
(a)

(b)

Figure 2. (a) The original FTIR spectral band (after subtracting the D_2O spectra) of the roots PM vesicles incubated with 200 μM H_2O_2, Fe^{2+}, and Fe^{3+} at 4°C for 30 min (from the top Spectral line to the bottom Spectral line were indicated the control, 200 μM H_2O_2, 200 μM Fe^{2+}, and 200 μM Fe^{3+} treatment spectral line respectively). (b) The contents of ester (shaded columns) and amide I (open columns) in membrane proteins and lipids damaged by 200 μM H_2O_2, Fe^{2+}, and Fe^{3+} treated at 4°C for 30 min.

and 61% than those of untreated the roots PM respectively. The roots PM lipid content had remained only 11% of the ester content of untreated the roots PM vesicles when treated with 200 μM H_2O_2 and Fe^{2+}, which decreases to only 2% for the 200 μM Fe^{3+} treatments. It is suggested that Fe^{3+} damage had a stronger effect on the membrane protein and lipid than the damage caused by Fe^{2+}. We can also found that the greatest damage to the membrane proteins was caused by H_2O_2.

3.3. The Protein Secondary Structure Conformation of the Root PM Damaged by H_2O_2 and Fe

The original FTIR spectral bands (**Figure 2(a)**) often generated complex multi-component bands that over-

lapped into a broad unresolved absorption. To quantitatively analyze the change in intensities of the amide I band, the IR spectra of the roots PM used Fourier self-deconvolution and second-derivative spectral mathematical calculated. After the IR spectra of the roots PM were resolved with Fourier self-deconvolution and second-derivative treatment by the software OMNIC 6.0, it was found that several peaks belonged to the amide I bands, but the two main peaks of amide I band at 1656 cm^{-1} and 1638 cm^{-1} intensity were the two strongest absorbance intensity bands.

The IR spectra of the roots PM were curve-fitted using Origin 7.0 software with an appended PFM (peak fitting maximum) function. The Gaussian peak shape was used to fit the spectrum collected at each time point, and the all-treatment curve-fitting results are shown in **Figure 3**. According to Byler's [20] study on 10 - 20 known lipid membrane proteins' secondary structures using X-rays, combined with these the roots PM-FTIR spectral result, we were able to assign component bonds to several chemical functions. The main amide I band, which is located at 1656 cm^{-1}, belongs to α-helix, whereas the 1638 cm^{-1} band belongs to β-sheets.

The amide I band has been widely used to reveal the secondary structure of the proteins. From the spectrum, as can be seen in **Figure 3(a)**, the amide I band can be decomposed into two main bands clearly located at 1656 cm^{-1} and 1638 cm^{-1}. The amide band located at 1656 cm^{-1} belongs to the α-helix, whereas the 1638 cm^{-1} band belongs to β-sheets [19]. The relative band area percentages of these two positions of amide I bands (1656 and 1638 cm^{-1}) reflect the degree of protein second structure composed. In general the higher of percenttage of α-helix, the greater the stability of the proteins, so **Figure 3(b)** shows that compared with the control untreated PM sample, the protein construction of α-helix decreased from 70% to 56%, 40% and 38% in amide I after damage caused by Fe^{2+}, H_2O_2, and Fe^{3+} solution respectively , and thus the percentage of β-sheet construction increased from 30% to 44%, 60% and 62% in amide I after damage caused by 200 μM Fe^{2+}, H_2O_2, and Fe^{3+} solution. These results indicate that the composition of α-helix in the secondary structure of protein changed a lot because of the attack by Fe^{2+}, H_2O_2, and Fe^{3+}, which indicate that the roots PM protein conformation had changed, suggest that the membrane protein function was affected by physical state under oxidation damage.

3.4. The P=O Bond in the Roots PM Was Diminished

In these experiments, the 1260 cm^{-1} and 1050 cm^{-1} absorption bands indicate systemic and antisystemic stretching vibrations of the content of P=O in the roots PM lipids. The results (**Figure 4**) showed that these were
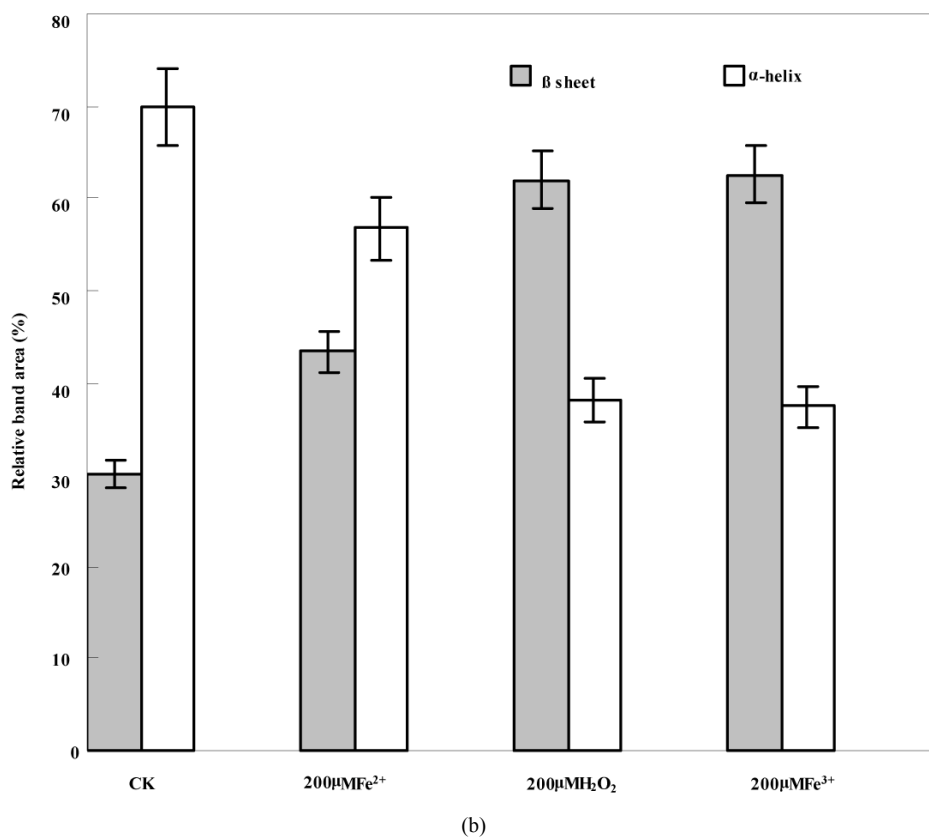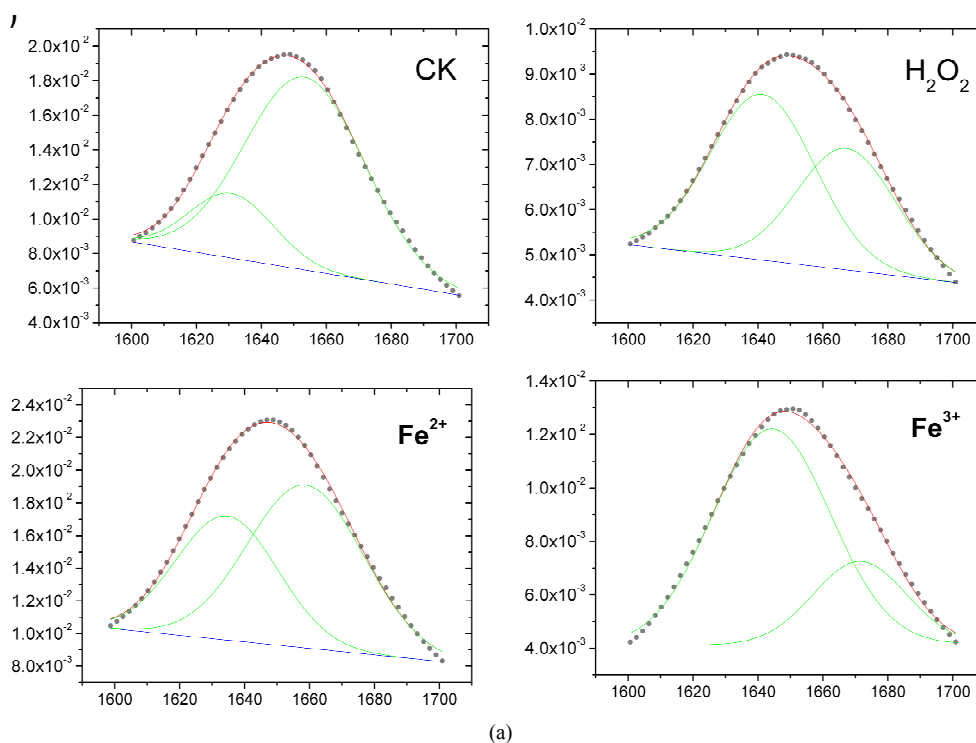
(a)

(b)

Figure 3. (a) The curve fitting of amide I (1600 - 1700 cm^{-1}) of the roots PM vesicles incubated with 200 μM H$_2$O$_2$, Fe^{2+}, and Fe^{3+} (from the top to the bottom); (b) The change in the secondary structure of membrane protein before and after damage by the oxidant. The protein secondary structure of two main bands of 1638 cm^{-1} (*β*-sheets, shaded columns) and 1656 cm^{-1} (*α*-helix, open columns), showing percentage area of whole amide I (1600 - 1700 cm^{-1}) occupied.
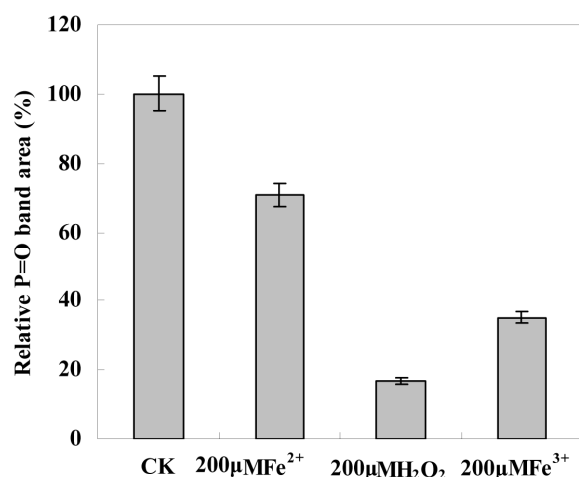
Figure 4. The content of P=O $\left(A_{(1251\,cm^{-1}+1056\,cm^{-1})}\right)$ in membrane lipids damaged by 200 μM H_2O_2, Fe^{2+}, and Fe^{3+} treated at 4°C for 30 min (spectral normalized results).
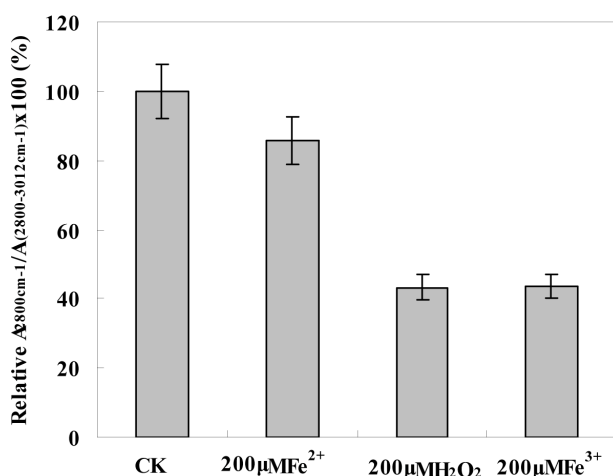
Figure 5. The value of $A_{3012\,cm^{-1}}/A_{(2800-3030\,cm^{-1})}$ of membrane lipids damaged by 200 μM H_2O_2, Fe^{2+}, and Fe^{3+} treated at 4°C for 30 min.

strongly damaged (reduced to about 20% and 40% of the untreated control PM sample) by H_2O_2 and Fe^{3+}, but only weakly damaged by Fe^{2+} oxidation. The main damaged section was on the polar of the lecithin of the roots PM, so these changes in the molecular structure of the top section of lecithin leads to a diminishing of the fluidity of the roots PM. This could be a possible reason why the roots PM fluidity decreased sharply with 200 μM H_2O_2 treatment, but was only affected slightly by 200 μM Fe^{2+} (**Figure 1**).

3.5. The C=C Bond in the Roots PM Was Diminished

The roots PM lipids in the FTIR spectral line exhibit

several absorbance peaks: 2800 - 3030 cm^{-1} assigned to C-H stretching vibration regions; 2957 cm^{-1} and 2935 cm^{-1} assigned to CH_3 and CH_2 antisymmetric stretching vibration regions, respectively; and 2873 cm^{-1} and 2853 cm^{-1} assigned to CH_3 and CH_2 symmetric stretching vibration regions, respectively, 3012 cm^{-1} belong to C=C stretching vibration region. According to other reports [9,12], the ratio of $A_{3012\,cm^{-1}}/A_{(2800-3030\,cm^{-1})}$ is attributed to the amount of C=C bond in membrane lipids. The amount of C=C in the roots PM lipids treated by H_2O_2, Fe^{2+}, and Fe^{3+} diminished to 15%, 60%, and 20%, respectively, of the amounts found in untreated the roots PM (**Figure 5**). This means that most of the C=C of the side of the roots PM unsaturated fatty acid were oxidized to C-C. The molecules of the roots PM lipid acid piled more tightly than those of the undamaged the roots PM vesicles, thus reducing the fluidity of the roots PM vesicles.

4. DISCUSSION

In this study, we found that FTIR spectroscopic analysis reveal large changes in the secondary structure of plant cell membrane protein associated with the oxidant iron and H_2O_2. The protein and lipid content of the roots PM changed with oxidant damaged, and the protein second structure of α-helix and β-sheets composed completely different than untreated the roots PM. Oxidant injury results in a more strongly unstable structure that has a significantly reduced fluidity of the roots PM.

Under hostile environmental stress, the fluidity of the roots PM would decrease [21,22]. Our experiment result was similar to that of Qiu's [21], who reported that a $FeSO_4$ solution injured erythrocyte membranes and induced changes in their protein structure; the main cause being that OH· oxidation damage impaired the binding power of the roots PM proteins' intramolecular and intermolecular hydrogen. This is the main reason for the decline in the fluidity of the roots PM.

Qiu [21] reported that the roots PM vesicles were getting smaller and the membrane fluidity and surface charge density were decreased under osmotic stress, suggesting that the membrane protein function was affected by the physical state under osmotic stress. In our experiments gave a similar result with his.

Yang [10] reported that iron caused a decrease in plasma protein thiol (P-SH), and Fe^{3+} brought a higher degree of oxidation in thiol groups than Fe^{2+} at the same concentration. The decreased α-helix in the amide I of the roots PM give a reason for the attack by Fe^{2+}, H_2O_2, and Fe^{3+}. There was a positive correlation ($R^2 = 0.8775$) between relative H$^+$-ATPase activity and the corresponding relative band area percentage of α-helix in the amide I region.

Our results showed that a significant decrease in α-helix, and a relative increase in the β-sheet occurred (**Figure 3(b)**) when the plasma membrane was incubated with 200 μM H_2O_2, $FeSO_4$, and $FeCl_3$. $FeCl_3$ induced a greater decline in the α-helix than $FeSO_4$; the effect of H_2O_2 treatment induced result was intermediate between the $FeCl_3$ and $FeSO_4$ treatments (**Figure 3(b)**). And a stronger degree change made to lipid section (**Figures 4 and 5**). These results indicated that the damage on plasma membrane protein structure were due to the specific action of H_2O_2, Fe^{2+}, and Fe^{3+}, indicating that the roots PM physical state changed from stable to unstable state under these treatments.

According to Yang research [10] has shown that $FeCl_3$ induced stronger inhibition in the H^+-ATPase activity than $FeSO_4$ did at progressive concentrations of 100, 200, and 300 μM. Investigation of the effects of various reactive oxygen species scavengers on the iron-mediated inhibition of H^+-ATPase activity indicated that hydroxyl radicals (HOH) and hydrogen peroxide (H_2O_2) might be involved in the Fe^{2+}-mediated decrease in the roots PM H^+-ATPase activity. What is the reason of the H^+-ATPase activity inhibited? From our study, the main reason may be that they directly changed the content of α-helix in the roots PM protein secondary structure.

This means that carbonyl at the SN-2 section stretching vibration becomes aggravated. This is due to changes in the orientation of the glycerol skeletal region; that is to say the C=O increases at close to the top polar section and changes the structure of the ester polar section. The orientation of C=O changes, and maybe also the P=O changes, and the main damaged section was on the polar top of lecithin of the roots PM.

After damage by H_2O_2, $FeSO_4$, and $FeCl_3$, the changed content of P=O bonds means they are changed at the polar head region, finally decreasing the roots PM's molecular fluidity. The decrease in the amount of C=C makes the degree of instauration of the CH chains decreased.

5. ACKNOWLEDGEMENTS

REFERENCES

[1] Mittler, R. (2002) Oxidative stress, antioxidants and stress tolerance. *Trends Plant Science*, **7**, 5-10.

[2] Davies, K.A., Sharon, W.L. and Pacifici, R.E. (1987) Protein damage and degradation by oxygen radicals. I. General aspects. *Journal Biology Chemistry*, **262**, 9914-9920.

[3] Stadtman, E.R. (1986) Oxidation of proteins by mixed-function oxidation systems: Implication in protein turn-over, ageing and neutrophil function. *Trends Biochemistry Science*, **11**, 11-12. doi:10.1016/0968-0004(86)90221-5

[4] Wolff, S.P., Garner, A. and Dean, R.T. (1986) Free radicals, lipids and protein degradation. *Trends Biochemistry Science*, **11**, 27-31. doi:10.1016/0968-0004(86)90228-8

[5] Raven, J.A. (1990) Predictions of Mn and Fe use efficiencies of plant growth with different energy, carbon and nitrogen sources. *New Phytologist*, **109**, 279-287. doi:10.1111/j.1469-8137.1988.tb04196.x

[6] Ponnamperuma, F.N., Bradfield, J.F. and Peech, M. (1955) Physiological disease of rice attributable to iron toxicity. *Nature*, **175**, 275. doi:10.1038/175265a0

[7] Kneen, B.E., LaRue, T.A., Welch, R.M. and Weeden, N.F. (1990) Pleitropic effects of *brz*: A mutation in *Pisum sativum* (L.) cv "Sparke" conditioning decreased nodulation and increased ion uptake and leaf necrosis. *Plant Physiology*, **93**, 717-723. doi:10.1104/pp.93.2.717

[8] Briat, J.F., Forbis-Loisy, I., Grignon, N., Lobraux, S., Pascal, N., Savino, G., *et al.* (1995) Cellular and molecular aspects of iron metabolism in plants. *Biology Cell*, **84**, 69-81. doi:10.1016/0248-4900(96)81320-7

[9] Sills, R.H., Moore, D.J. and Mendelsohn, R. (1994) Erythrocyte peroxidation: Quantitation by fourier transform infrared spectroscopy. *Analytical Biochemistry*, **218**, 118-123. doi:10.1006/abio.1994.1149

[10] Yang, Y.L., Zhang, F., He, W.L., Wang, X.M. and Zhang L.X. (2003) Iron-mediated inhibition of H^+-ATPase in plasma membrane vesicles isolated from wheat roots. *Cellular and Molecular Life Sciences*, **60**, 1249-1257.

[11] Goormaghtigh, E., Raussens, V. and Ruysschaert, J.M. (1999) Attenuated total re£ection infrared spectroscopy of proteins and lipids in biological membranes. *Biochimica ET Biophysica Acta*, **1422**, 105-185. doi:10.1016/S0304-4157(99)00004-0

[12] Phelan, A.M. and Lange, D.G. (1991) Ischemia/reperfusion-induced changes in membrane fluidity characteristics of brain capillary endothelial cells and its prevention by liposomal-incorporated superoxide dismutase. *Biochemistry Biophysical Acta*, **1067**, 97. doi:10.1016/0005-2736(91)90030-C

[13] Timasheff, S.N., Susi, H. and Stevens, L. (1967) Infrared spectra and protein conformations in aqueous solutions II. Survey of globular proteins. *The Journal of Biological Chemistry*, **242**, 5467-5473.

[14] Kasamo, K. and Sakibara, Y. (1995) The plasma membrane reconstitution into liposomes and its regulation by phospholipids. *Plant Science*, **111**, 117-131. doi:10.1016/0168-9452(95)04224-I

[15] Widell, S., Lundborg, T. and Christer, L. (1982) Plasma membranes from oats prepared by partition in an aqueous polymer two-phase system. *Plant Physiology*, **70**, 1429-1435. doi:10.1104/pp.70.5.1429

[16] Bradford, M. (1976) A Rapid and sensitive method for the quantitation of microgram quantities of protein utilizing the principle of protein-dye binding. *Analytical Biochemistry*, **72**, 248-254. doi:10.1016/0003-2697(76)90527-3

[17] Zhang, W.H., Chen, Q. and Liu, Y.L. (2002) Relationship between H^+-ATPase activity and fluidity of tonoplast in

barley roots under NaCl stress. *Acta Botanical Sinica*, **44**, 292-296.

[18] Witold, K., Surewicz, J., Mantsch, H. and Chapman, D. (1993) Determination of protein secondary structure by fourier transform infrared spectroscopy: A critical assessment? *Biochemistry*, **32**, 19.

[19] Zhao, X., Shi, Y., Chen, L., Sheng, F. and Zhou, H. (2011) Secondary structure changes and thermal stability of plasma membrane proteins of wheat roots in heat stress. *American Journal of Plant Sciences*, **2**, 816-822. doi:10.4236/ajps.2011.26096

[20] Byler, D.M. and Susi, H. (1986) Examination of the secondary structure of proteins by deconvolved FTIR spectra. *Biopolymers*, **25**, 469-487. doi:10.1002/bip.360250307

[21] Qiu, Q.S. and Su, X.F. (1998) The influence of extra cellular side Ca^{2+} on the activity of the plasma membrane H^+-ATPase from wheat roots. *Australian Journal Plant Physiology*, **25**, 923-928. doi:10.1071/PP98036

[22] Qiu, Q.S. (1999) Influence of Osmotic stress on the lipid physical states of plasma membrane from wheat roots. *Acta Botanical Sinica*, **41**, 161-165.